

High lipophilicity of *meta* Mn(III) *N*-alkylpyridylporphyrin-based SOD mimics compensates for their lower antioxidant potency and makes them equally effective as *ortho* analogues in protecting SOD-deficient *E. coli*

Ivan Kos,¹ Ludmil Benov,² Ivan Spasojevic,³, Julio S. Reboucas,¹ Ines Batinic-Haberle^{1*}

Departments of Radiation Oncology¹, and Medicine³, Duke University Medical School, Durham, NC 27710, USA and Department of Biochemistry², Faculty of Medicine, Kuwait University, Safat 13110, Kuwait

Supplemental Information

Content

<i>Experimental</i>	S1
General	S1
ESI-MS	S2
Uv/vis spectra	S2
Electrochemistry	S2
Porphyrin synthesis	S2
<i>E. coli</i> growth	S2
Accumulation of Mn porphyrin in <i>E. coli</i>	S2
<i>Tables</i>	S3
Table 1S – uv/vis characteristics of MnTE-3-PyP and MnTnPr-3-PyP	S3
<i>Figures</i>	S3
Figure 1S - SOD-deficient <i>E. coli</i> growth as a function of MnP concentration	S3
Figure 2S - Toxicity of MnP to AB1157 in M9CA medium	S4
Figure 3S - Toxicity of MnP to AB1157 in 5 amino acid medium	S5
Figure 4S - Calibration curve for calculation of MnP accumulation in <i>E. coli</i>	S5
Figure 5S - Accumulation of MnP in membranes of <i>E. coli</i>	S5
Figure 6S - Accumulation of MnTnPr-2(or 3)-PyP in cytosol and membranes <i>E. coli</i> - uv/vis spectra	S6
Figure 7S - Accumulation of MnTnBu-2(or 3)-PyP in cytosol and membranes <i>E. coli</i> - uv/vis spectra	S6
Figure 8S - Accumulation of MnTnPr-2(or 3)-PyP in cytosol and membranes <i>E. coli</i> - uv/vis spectra	S7
Figure 9S - Accumulation of MnTnPr-2(or 3)-PyP in whole <i>E. coli</i> –uv/vis spectra	S7

Experimental

General. Xanthine and equine ferricytochrome *c* (lot no. 7752) were from Sigma, whereas xanthine oxidase was prepared by R. Wiley¹⁸ and was a gift from K.V. Rajagopalan. MnCl₂·4H₂O was purchased from J. T. Baker. Anhydrous *N,N*-dimethylformamide (DMF, Sigma-Aldrich Chemical Co) was kept over 4 Å molecular sieves. Ethyl ether (anhydrous), acetone and chloroform were from EMD. NH₄PF₆ (>99.9999% purity) was from Advance Research Chemicals, Inc. KNO₃ and methanol were from Mallinckrodt. Acetonitrile was from Fisher Scientific. Silica gel TLC plates (Z122777-25EA, Batch#3110), tetrabutylammonium chloride and ethyl *p*-toluenesulfonate were purchased from Sigma-Aldrich. The *n*-propyl ester of *p*-toluenesulfonic acid was purchased from TCI America. All other chemicals and solvents were of analytical grade and used without further purification.

Electrospray ionization mass spectrometric analyses (ESI-MS) were performed as described elsewhere²⁶ on an Applied Biosystems MDS Sciex 3200 Q Trap LC/MS/MS spectrometer at Duke Comprehensive Cancer Center, Shared Resource Pharmaceutical Services PK/PD Labs; all samples of ~5 μM concentration were prepared in a H_2O -acetonitrile (1:1, v/v; containing 0.1 % v/v HFBA) mixture and infused for 1 min at 10 $\mu\text{L}/\text{min}$ into the spectrometer (curtain gas = 20 V; ion spray voltage = 3500 V; ion source = 30 V; T = 300 °C; declustering potential = 20 V; entrance potential = 1 V; collision energy = 5 V; gas = N_2).

UV/vis spectra were recorded in H_2O at room temperature ($25 \pm 1^\circ\text{C}$) on a Shimadzu UV-2501PC spectrophotometer with 0.5 nm resolution.

Electrochemistry. The cyclic voltammetry was carried out on a CH Instruments Model 600 Voltammetry Analyzer. A three-electrode system consisted of a 3 mm-diameter glassy carbon button working electrode (Bioanalytical Systems), the Ag/AgCl reference electrode, and a Pt auxiliary electrode was used in a small volume cell (3.0 mL). Helium-purged solutions contained 0.05 M phosphate buffer (pH 7.8), 0.1 M NaCl, and 0.5 mM Mn porphyrin. The scan rates were 0.01-0.5 V s^{-1} , typically 0.1 V s^{-1} . The potentials were standardized against $\text{Mn}^{\text{III}}\text{TE-2-PyP}^{5+}$ (chloride salt) ($E_{1/2} = +228 \text{ mV vs NHE}$).

Porphyrin. All MnT(alkyl)-2 or 3-PyP were prepared as previously reported. N-alkylation. N-alkylation was faster with sterically less hindered *meta* isomers than with their *ortho* analogues.^{2,19} Typically, to a 100 mg of $\text{H}_2\text{T-3-PyP}$ (Frontier Scientific) in 20 mL *N,N'*-dimethylformamide at 100°C were added 4 mL of the corresponding *p*-toluenesulfonate. Reaction was followed by thin-layer chromatography on silica gel TLC plates using 8:1:1 acetonitrile: KNO_3 -saturated $\text{H}_2\text{O}:\text{H}_2\text{O}$ as mobile phase. Single spot (lack of atropoisomers as compared to *ortho* porphyrins) marked the completion of N-alkylation. Upon completion, reaction mixture was poured in a separatory funnel containing 200 ml each of water and chloroform and shaken well. The chloroform layer was discarded and extraction with CHCl_3 was repeated several times. The aqueous layer was filtered and the porphyrin was precipitated as PF_6^- salt by dropwise addition of a concentrated aqueous solution of NH_4PF_6 , until no further precipitate was formed. Precipitate was filtrated and thoroughly washed with diethyl ether. Dried precipitate was dissolved in acetone, filtered and precipitated as chloride salt by the addition of acetone solution of tetrabutylammonium chloride. The precipitate was washed thoroughly with acetone and dried in vacuum at room temperature. Metallation. 20-fold excess MnCl_2 is added to a pH 12.5 solution of porphyrins at 25 °C. Alike N-alkylation, metallation occurs much faster with *meta* than with *ortho* isomers due to the lack of steric hindrance, usually within few hours at room temperature; the duration depends upon the length of the alkyl chains. The reaction progress was followed by uv/vis spectroscopy and TLC (8:1:1=acetonitrile: KNO_3 -saturated $\text{H}_2\text{O}:\text{H}_2\text{O}$) until the disappearance of both Soret band and fluorescence of the metal-free porphyrin. Upon completion, the suspension (excess of free Mn in the form of Mn oxo/hydroxo species) was filtered off, and the filtrate was precipitated with aqueous solution of NH_4PF_6 and washed with ether. Precipitate was dissolved in acetone, precipitated with an acetone solution of tetrabutylammonium chloride and the resulting precipitate was washed with acetone. The $\text{PF}_6^-/(\text{aq})/\text{Cl}^-/(\text{acetone})$ precipitation procedure was repeated twice to assure removal of free manganese.

E. coli growth. *Escherichia coli* strains used in this study were AB1157, wild type (*F-thr-1*; *leuB6*; *proA2*; *his-4*; *thi-1*; *argE2*; *lacY1*; *galK2*; *rpsL*; *supE44*; *ara-14*; *xyl-15*; *mtl-1*; *tsx-33*), and JI132, SOD-deficient, $\text{sodA}^-\text{sodB}^-$ (same as AB1157 plus (*sodA::mudPR13*)25 (*sodB-kan*)1- Δ 2). Both strains were obtained from J. A. Imlay [Imlay, J. A.; Linn, S. Mutagenesis and stress responses induced in *Escherichia coli* by hydrogen peroxide. *J. Bacteriol.* **1987**, *169*, 2967–2976]. The experiments were carried out in triplicates as described in detail in ref 31. Briefly, cultures were grown aerobically in either casamino acid (M9CA) medium or in minimal 5 amino acid (L-leucine, L-threonine, L-proline, L-arginine, L-histidine) medium in 96-well plates in a shaking thermostat at $37 \pm 0.1^\circ\text{C}$ and 200 rpm. The effect of Mn porphyrins on the growth of the SOD-deficient strains was followed turbidimetrically at 700 nm (to minimize the interference of compounds studied) and compared to the growth curves of both strains in the absence of Mn porphyrin (controls). The potential toxicity of the compounds was followed in minimal 5 amino acid as well as in rich M9CA medium. Deionized water was used throughout the study.

Accumulation of Mn porphyrins in E. coli. Two experiments were performed. In a 1st experiment the cytosolic and membrane fractions were separated and analyzed as described in main text. In 2nd experiment the wild type AB1157 was grown exactly as in 1st experiment. The cells were then washed with ice-cold M9CA medium, resuspended in the same medium and kept on ice. Spectra of whole cells were

recorded using suitably diluted cell suspensions. All experiments were done in triplicates.

Under aerobic conditions and in the absence of reductants, MnPs are stabilized with Mn being in +3 oxidation state. Due to the reductive cellular environment, inside the respiring cell, MnPs exist predominantly as Mn^{II}P. However, it is close to impossible to prevent oxidation of Mn^{II}P to Mn^{III}P during manipulation of the cells and thus to assess unambiguously the oxidation state of Mn within intact cells. Even after cell disruption, the spectra of processed cytosolic and membrane fractions (1st Experiment) still showed significant levels of reduced Mn^{II}P, which suggests extensive reduction of MnP within respiring cell; reduction was more obvious with the suspension of membrane fraction. Two maxima were seen, one related to oxidized Mn^{III}P at around 454 nm for *ortho* and 460 nm for *meta* isomers, the other related to reduced Mn^{II}P at shorter wave lengths (Figure 6S-8S). Again, with the whole cell preparation of propyl isomers (2nd experiment) two maxima were seen: one related to oxidized Mn^{III}P (at 453 nm for *ortho* and 459 nm for *meta* isomer), the other related to the reduced Mn^{II}P at shorter wave lengths (448 nm for *ortho* and 452 nm for *meta* porphyrin) (Figure 9S). To note, upon centrifuging the M9CA medium containing cells and before any manipulation, the cellular pellet was greenish, which is a clear sign of the presence of porphyrin in reduced state, Mn^{II}P (oxidized Mn^{III}P is brown-reddish). We adopted two approaches to calculate the levels of MnPs in cytosolic and membrane fractions: (a) using the molar absorptivities and (b) using area below the Soret band. Both approaches offered same conclusions, but the latter appeared to be a more correct strategy as it accounted for both oxidized and reduced porphyrin. We calculated the levels of porphyrins using a calibration curve where we plotted the area below Soret band vs concentration of either *ortho* or *meta* porphyrins (Figure 2S).

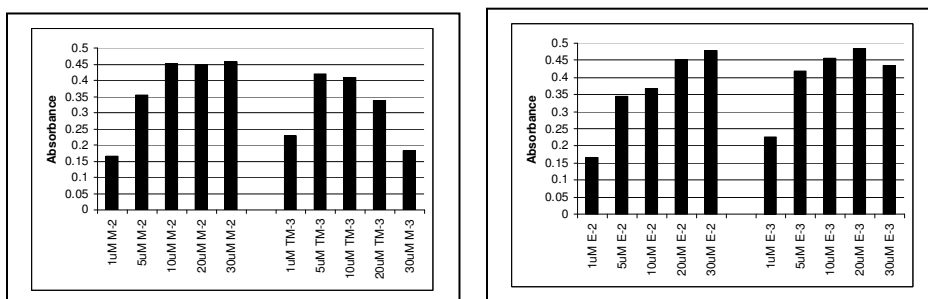
Table 1S. Wave lengths (λ) of absorption maxima (nm), and molar absorption coefficients of aqueous solutions of chloride salts of metal-free porphyrins and their Mn(III) complexes synthesized in this work ($T = 25 \pm 1^\circ\text{C}$) given as \log values. The data for other compounds can be found elsewhere.^{2,18,19}

Porphyrin	λ_{max} ($\log \epsilon^a$)
H ₂ TE-3-PyP	830.0(2.93); 582.0(3.82); 515.0(4.25); 417.0(5.52); 320.0(4.28); 261.0(4.38)
H ₂ TnPr-3-PyP	848.0(2.89); 581.0(3.79); 514.0(4.26); 417.0(5.55); 318.0(4.26); 264.0(4.34)
MnTE-3-PyP	837.0(2.40); 766.-(3.37); 674.0(3.25); 557.0(4.16); 502.0(3.85); 460.0(5.19); 395.0(4.78); 373.0(4.74); 260.0(4.60); 214.0(4.77)
MnTnPr-3-PyP	835.5(2.47); 757.0(3.33); 671.5(3.39); 558.0(4.12); 500.0 (3.83); 460.0(5.14); 395.0(4.66); 373.0(4.69); 261.0(4.57); 213.0(4.76)

^aMolar absorption coefficient ($\text{M}^{-1} \text{cm}^{-1}$) were determined in water at room temperature ($\pm 5\%$). λ_{max} (nm) were determined with errors within 0.5 nm.

Figures

Figure 1S. SOD-deficient *E. coli* growth as a function of the concentration of *ortho* (2) and *meta* (3) isomers of Mn(III) *N*-alkylpyridylporphyrins. The ascending absorbance with hexyl porphyrin from 5 to 30 μM is due to the contribution of the porphyrin absorbance at 700 nm.



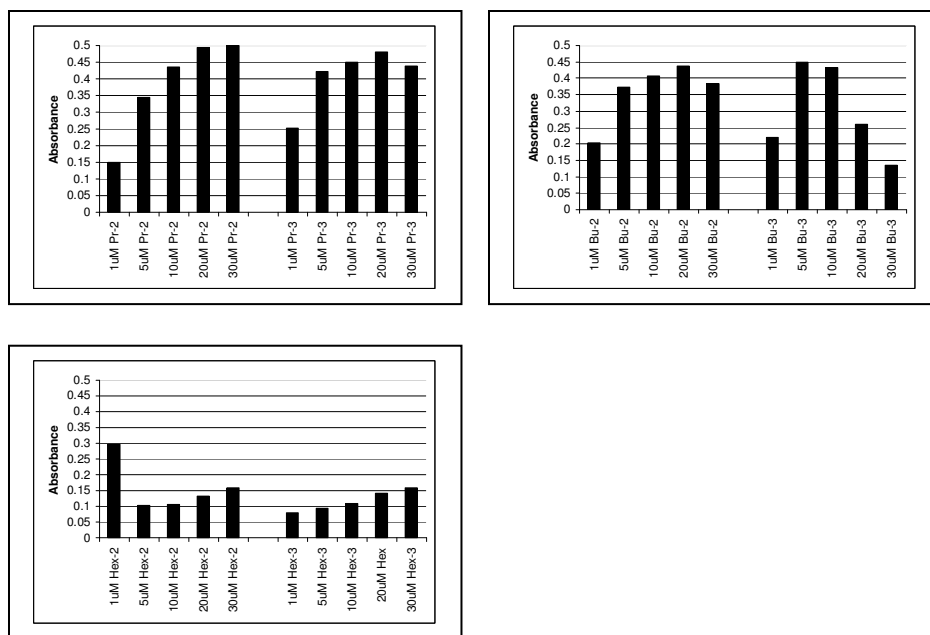


Figure 2S. The aerobic growth of SOD-proficient *E. coli* AB1157 in M9CA rich medium in the presence of *ortho*(2) and *meta*(3) analogues followed in terms of absorbance at 700 nm and shown here at 14th hour of growth and at 20, 30, 60 and 100 μM concentrations for methyl to butyl porphyrins (A) and at 12th hour of growth for 0.5 to 20 μM hexyl analogues (B). The growth of SOD-proficient *E. coli* AB1157 in the absence of Mn porphyrins is also shown. Bars represent mean \pm S.E.

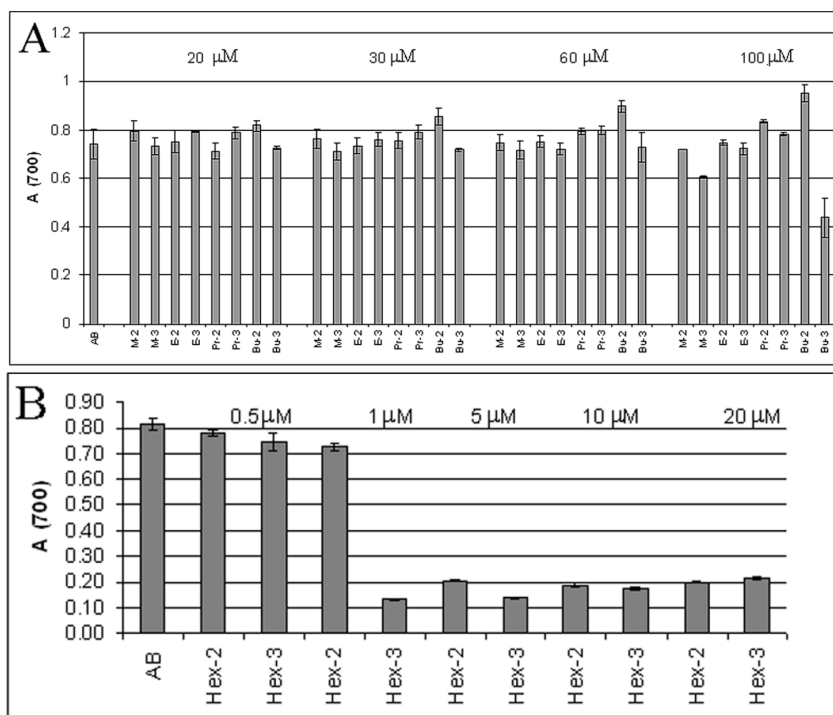


Figure 3S. The aerobic growth of SOD-proficient *E. coli* AB1157 in 5 amino acid minimal medium in the presence of *ortho*(2) and *meta*(3) analogues shown here at 18th hour of growth and at 20 μ M concentrations. The growth of SOD-proficient *E. coli* AB1157 in the absence of Mn porphyrins is shown also. The growth of *E. coli* was followed in terms of absorbance at 700 nm. Bars represent mean \pm S.E.

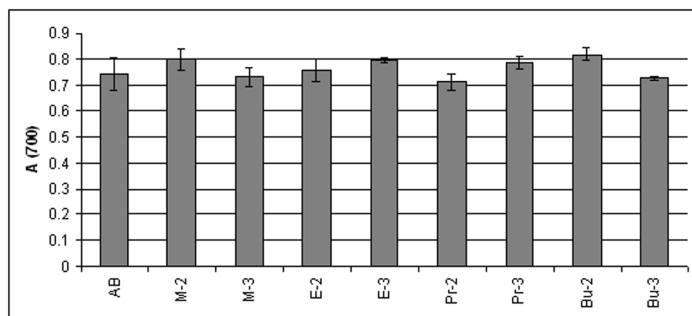


Figure 4S. Calibration curve for the determination of MnP in cytosolic and membrane fractions of *E. coli*. The calibration curve was used to make Figure 6 in main text of the manuscript and Figure 3S in the Supplemental. The area below Soret band was plotted vs MnP concentration. Same areas were obtained whether *ortho* or *meta* isomers were used for calibration curve.

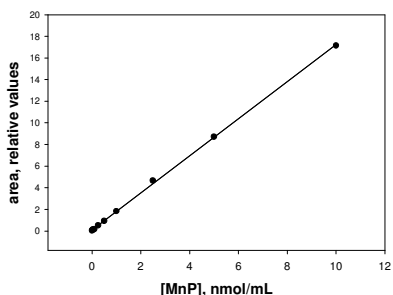


Figure 5S. Levels of *ortho* and *meta* isomers of Mn(III) *N*-alkylpyridylporphyrins in membrane fractions of (A) wild type AB1157 and (B) SOD-deficient *E. coli* after 1 hour of incubation with MnPs (5 μ M) in M9CA medium. Data are presented as nmol of MnP per mg of protein vs number of carbon atoms (nC) in pyridyl alkyl chains. Bars represent mean \pm S.E.

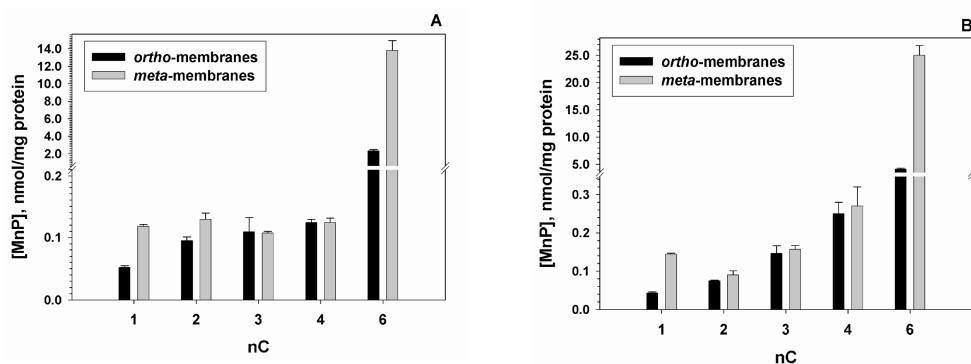


Figure 6S. Accumulation MnTnPr-2,3-PyP in JI132 *E. coli* after 1 hour of aerobic incubation with MnPs (5 μ M) in M9CA medium. The spectra of oxidized Mn^{III}P in homogenate shows Soret bands at ~454 nm for *ortho* and ~460 nm for *meta* isomers. Shift of Soret bands to lower waver lengths indicates a contribution of the reduced Mn^{II}P species.

A) Membranes: a) *ortho* (454.0 nm); b) *meta* (453.4 and 459.8 nm)

B) Cytosol: a) *ortho* (448.6 nm); b) *meta* (458.6 nm)

Practically the same pattern of accumulation of MnTnPr-2-PyP and MnTnPr-3-PyP in AB 1157 *E. coli* was found (not shown).

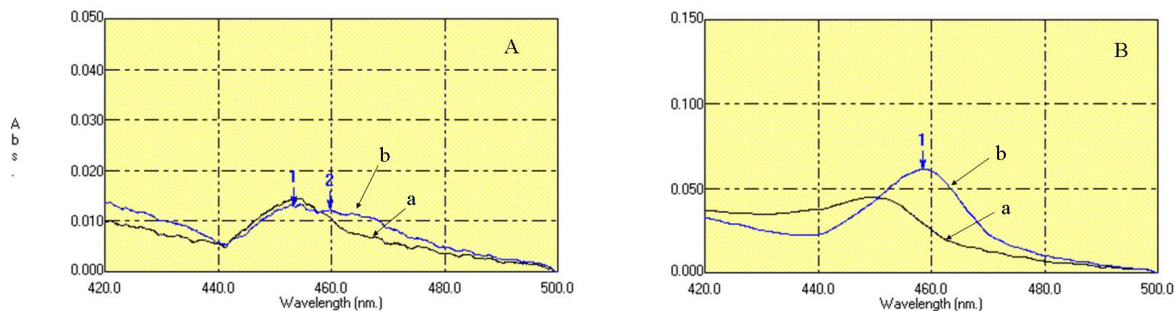


Figure 7S. Accumulation MnTnBu-2,3-PyP in JI132 *E. coli* after 1 hour of aerobic incubation with MnPs (5 μ M) in M9CA medium. Shift of Soret bands to lower waver lengths indicates a contribution of the reduced Mn^{II}P species.

A) Membranes: a) *ortho* (454.0 nm); b) *meta* (455 and 463.5 nm)

B) Cytosol: a) *ortho* (448.0 nm); b) *meta* (458.8 nm)

The same pattern of accumulation of MnTnBu-2-PyP and MnTnBu-3-PyP in AB 1157 *E. coli* was found (not shown).

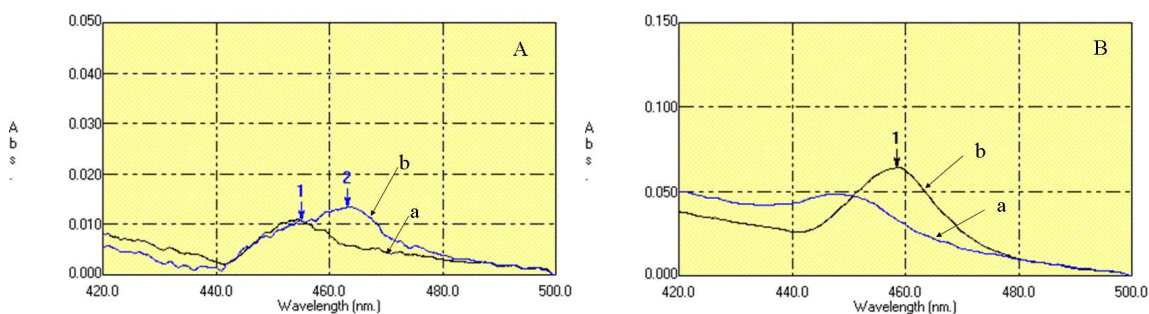


Figure 8S. Accumulation MnTnHex-2,3-PyP in JI132 *E. coli* after 1 hour of aerobic incubation with MnPs (5 μ M) in M9CA medium. Shift of Soret bands to lower waver lengths indicates a contribution of the reduced Mn^{II}P species.

A) Membranes: a) *ortho* (454.0 nm); b) *meta* (455 and 463.5 nm)

B) Cytosol: a) *ortho* (448.0 nm); b) *meta* (458.8 nm)

Similar accumulation of MnTnHex-2-PyP and MnTnHex-3-PyP in AB 1157 *E. coli* was observed (not shown).

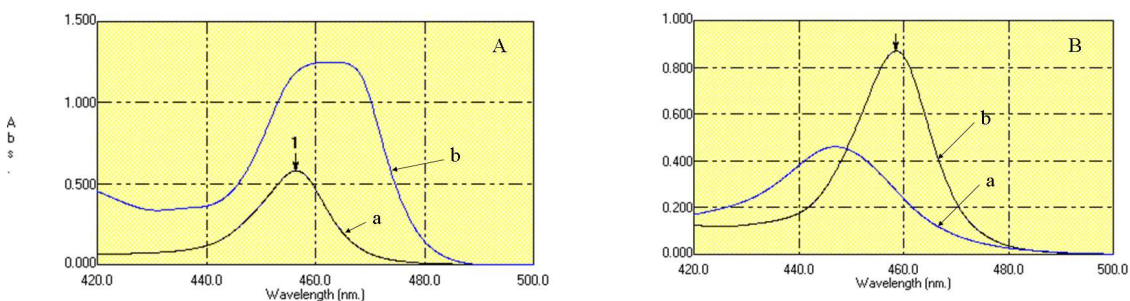


Figure 9S. Spectra of *meta* and *ortho* propyl Mn(III) *N*-alkylpyridylporphyrins in intact AB 1157 *E. coli* cells. A mid-log AB1147 culture was grown 1 hour in M9CA medium containing 5 μ M MnP. The cells were washed and resuspended in M9CA medium. Shift of Soret bands to lower waver lengths indicates a contribution of the reduced Mn^{II}P species.

a) - MnTnPr-2-PyP (peaks at 448 and 452 nm)

b) - MnTnPr-3-PyP (1 and 2 indicate Soret bands of reduced and oxidized *meta* MnP at 453 and 459 nm).

